Building Tomorrow's Society
Bâtir la Société de Demain

Fredericton, Canada
June 13 – June 16, 2018/ *Juin 13 – Juin 16, 2018*

FROM TOP-DOWN TO BOTTOM-UP APPROACHES TO RISK DISCOVERY: A PARADIGM SHIFT IN CLIMATE CHANGE IMPACTS AND ADAPTATION STUDIES RELATED TO THE WATER SECTOR

Seidou, Ousmane[1,3] and Alodah, Abdullah[1,2]
[1] University of Ottawa, Canada
[2] Qassim University, Saudi Arabia
[3] oseidou@uottawa.ca

Abstract: Healthy water resources are key to every nation's wealth and well-being. Unfortunately, stressors such as climate change, land-use shifts, and increased water consumption are threatening water availability and access worldwide. The pressure on water resources is projected to increase dramatically in the future and turn into a global crisis unless bold actions are taken. Researchers and practitioners are therefore under great pressure to develop methodologies and tools that can streamline projected changes into adaptation decisions. The vast majority of climate change adaptation studies use a top-down approach, which essentially consists of using of a limited set of climate change scenarios to discover future risks. However, recent research has identified critical limitations to that approach; for instance, even when multi-model multi-scenario projections are used, not all possible future conditions are covered and therefore plausible risks may be overlooked. There is also no established way to evaluate the credibility of a given projection scenario, making it a challenge to include them in a decision or design framework. The bottom-up approach (which consists of identifying risky situations using stochastically generated climate states then use projections to evaluate their likelihood in the future) was recently put forward to address the limitations of the top-down approach, but several issues remain unaddressed. This paper proposes a methodology that allows the generation of a large number of climate change projections by combining the outputs of weather generators to the outputs of regional climate models, and associate a likelihood to each projection. The new set of projections provide a better coverage of the risk space, and can therefore facilitate the implementation of the bottom-up approach. Applications on the Upper Niger and Bani River Basins in West Africa, implementing 20 regional climate models (RCMs) with two emission scenarios (RCPs), is presented.

1 INTRODUCTION

The scientific community recognizes climate change as one of the most pressing global issues and there is a pressure on researchers to develop methodologies and tools that can streamline projected changes into adaptation decisions. The problem is not new and thousands of researchers have already tried to tackle the problem using a 'top-down' approach, which essentially consists of using of a limited set of climate change scenarios to discover future risks. However, some critical limitations of that approach have been delineated recently; for instance, it has emerged that even when multi-model multi-scenarios projections are used, not all possible future conditions are covered and therefore plausible risks may be overlooked; yet there is also no established way to evaluate the credibility of a given projection scenario, making it a challenge to include them in a decision or design framework. The 'bottom-up' approach (which consist of identifying risky situations using stochastically generated climate states then use projections to evaluate

their likelihood in the future) the was recently put forward to address the limitations of the top-down approach but several issues remain unaddressed. A typical (and hypothetical) output of the bottom-up approach is presented on Figure 1. The risk on a watershed is measured using a water stress index, which is calculated as function of a range of future temperature changes (ΔT) and precipitation changes (ΔP). Climate change projections of ΔT and ΔP from a limited number of Regional Climate Models (RCMs) are plotted on the map to give an indication of the likelihood of a particular combination of ΔT and ΔP, and therefore the associated value of water stress.

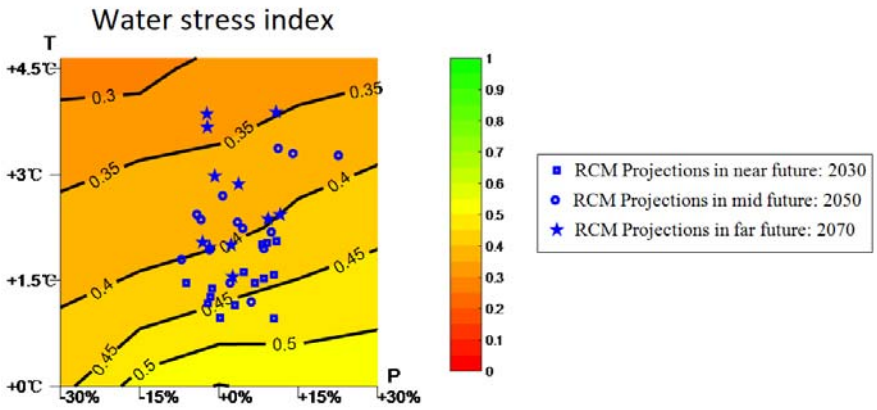

Figure 1: Typical output of the bottom-up approach to risk discovery

There are some obvious limitations to the usefulness of the above figure. The number of points representing the RCMs do not cover the entire space, meaning that the likelihood of certain combinations of ΔT and ΔP cannot be evaluated. All RCMs are treated equally, despite the fact that their performances are unequal in the historical period. A better approach would have been to provide each RCM output with a likelihood derived from how it fares on the historical period. This paper is an attempt to address the above issues using a novel stochastic method that would clone and perturb an initial set of climate change scenarios derived from climate models and generate new ones that would cover the range of variability observed on the historical period. The case study was performed on the Upper Niger and Bani River Basins (UNBB) in west Africa. At the outlet of the UNBB with lies the Inner Niger Delta (IND), which is the largest wetland in West Africa and source of income and food for at least 3 million people. A major concern for people in the area is the prospect that the delta would shrink to catastrophic states under climate change. First, a SWAT rainfall-runoff model is developed and calibrated on the UNBB. The outputs of an ensemble of 20 Regional Climate Models under scenarios RCP4.5 and RCP8.5 were downscaled and used to force the hydrological model to obtain projections of the hydrological cycle in the future. The KNN weather generator is then used to generate 250 random realizations of the historical climate. The 40 downscaled climate time series (from 20 RCMs using two RCP scenarios) were then rescaled to match the variance and/or mean of each realization of the weather generator, leading to 10200 climate projections in the future. A climate response function linking the average volume of water in the Inner Niger Delta to the statistical characteristics of precipitation in the area was calibrated using the SWAT model inputs and outputs on the historical period, and used to generate a high-resolution projection of the water volume in the Inner Niger Delta in the future. The projections are used to calculate the likelihood of particular values of the average volume of water in the IND.

2 MATERIAL AND METHODS

2.1 Study Area

The Niger River is the third longest African river and flows through 5 countries (Guinea, Mali, Niger, Benin, Nigeria), while draining runoff from four others (Burkina Faso, Ivory coast, Chad and Cameroun (Figure 1). The Inner Niger Delta (IND) in central Mali is a large wetland in an otherwise dry area that provides a multitude of ecosystem services to 3 million people. Two rivers flow in the IND: the Niger River at the North,

and the Bani River at the south. The area under investigation is the watershed of the Niger river at Diré station, just at the exit of the IND.

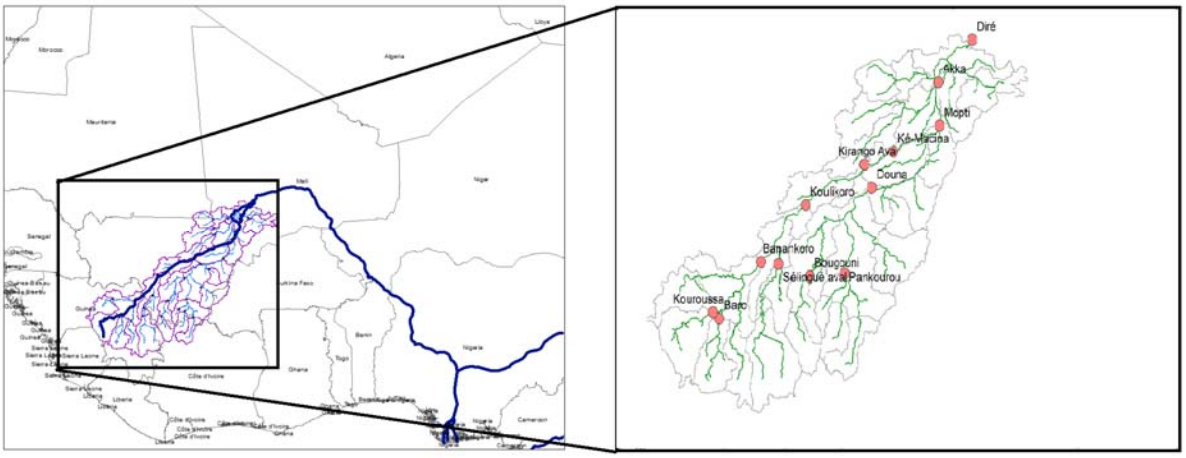

Figure 2: Geographic location of the UNBB

2.2 Hydrological Modeling

SWAT (Soil and Water Assessment Tool: Arnold et al., 1998) was used to develop a rainfall-runoff model of the UNBB. The model has 32 subwatersheds, 188 Hydrologic Response Units, and 4 reservoirs. The Delta is represented in the model by three reservoirs (at Mopti, Akka and Dré) in cascade since it is too large to be represented by a single reservoir. The SWAT reservoir routine was modified to account for the looped rating curves at the three stations in the IND. The other parameters of the model were derived from the following data sets:

1. Digital elevation model: Shuttle Radar Topography Mission (Jarvis et al., 2008),
2. Land use maps: Global Land Cover Facility (Bartholom and Belward, 2005),
3. Soil maps: Food and Agricultural Organization of the United Nations Organization for Education, Science and Culture (FAO/UNESCO, 2003),
4. Climate data from 1979 to 2012: WATCH-Forcing-Data-ERA-Interim (Weedon et al., 2017), and
5. Streamflow data: recorded streamflow at 14 hydrometric (Kouroussa, Baro, Selingué, Pankourou, Banakoro, Koulikoro, Douna, Kirango, Ke-Macina, Mopti, Akka and Diré) gauges throughout the watershed, obtained from the Malian and Guinean ministries of water resources.

The model was calibrated on the 1979-1997 period using the sequential uncertainty fitting (SUFI2) implemented in the SWAT-CUP program (Abbaspour, 2012), and validated on the 1998-2012 period. The Nash–Sutcliffe efficiency coefficient (NS) was used as an objective function in the calibration and validation phase:

$$[1]\ NS = 1 - \left[\frac{\sum_{i=1}^{n} (O_i - P_i)^2}{\sum_{i=1}^{n} (O_i - \bar{O})^2}\right]$$

where O stands for observed and P for predicted values, and $\bar{O}$ is the mean of the observed values. The calibration was done in a sequential manner starting from most upstream stations and moving towards the outlets.

2.3 Climate Statistics & Performance Indicator Spaces (R_T)

We are going to adopt the same framework as (Brown et al. 2012) where a climate state represented by a time series X_t is summarized by a subset of climate statistics v_T calculated over period T that are relevant to the problem under investigation (e.g. the mean, standard variation of precipitation and temperature). v_T belongs to a multidimensional space that will be called from now on the Climate Statistics Space (CSS). Elements of the CSS can be calculated any time series among observations, downscaled climate models outputs or stochastically generated time series. A climate state from the CSS will yield a level of risk and performance that is measured by a set of risk/performance indicators $\boldsymbol{R}_T$. $\boldsymbol{R}_T$ is obtained by feeding an impact model with time series, and belongs to another multidimensional space called the Risk and Performance Indicator Space (RPIS). A response function $\boldsymbol{f}$ (called the climate response function) can developed to map the climate statistics space to the performance state (i.e. $X_t = \boldsymbol{f}(v_T)$)). We also assume that following Brown et al. (2012), a weather generator was used to generate a large number of stochastic time series. Figure 1 illustrates the relationships between climate time series, climate statistics and risk/performance indicators in the bottom-up framework.

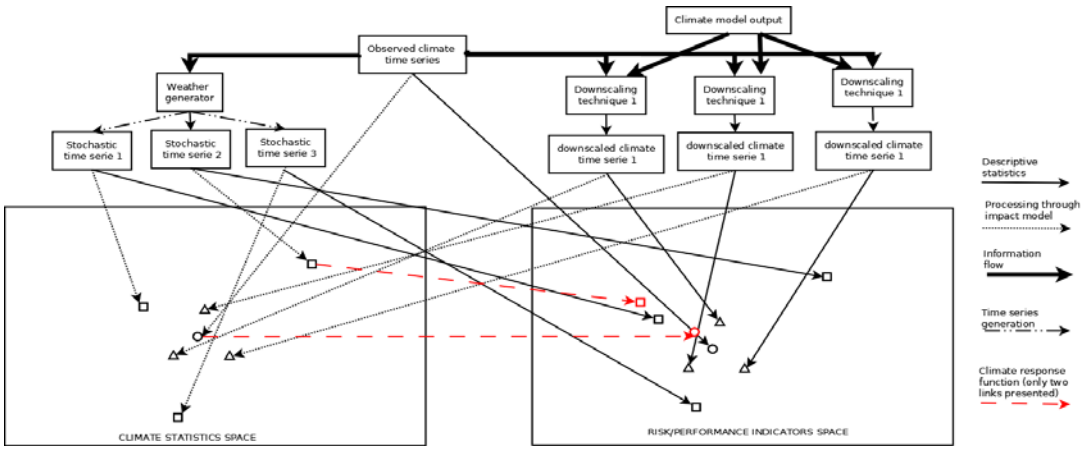

Figure 3: relationships between climate time series, climate statistics and risk/performance indicators in the bottom-up framework.

For the sake of simplicity, the RPIS is restricted to one dimensions corresponding to the average volume of water stored in the IND over a 30-years period.

2.4 Development of The Climate Response Function

While a lot of climate statistics can affect the volume of water in the IND, the dimensions of the CSS were restricted to two. The climate statistics to be included in the CSS were selected as follow:

a) The UNBB was divided into 7 regions shown on Figure 3

b) For each of the regions, and each month of the year M, 12 time series representing the cumulative precipitation on the region between month 1 and month M were generated from observed climate time series and downscaled climate time series. Each time series cover one of the following periods: 1986-2005, 2041-2070 and 2071-2100; These time series are denoted $CumPCP_t^{R,M,P}$ where R is the region (1 to 7), M is the month (1 to 12), P is the period (1986-2005, 2041-2070 or 2071-2100). t varies from 0 to the number of days in P.

c) For each of the regions, and each month of the year M, 12 time series representing the average temperature over the region between month 1 and month M were generated from observed climate time series and downscaled climate time series; Each time series cover one of the following periods:

1986-2005, 2041-2070 and 2071-20100; These time series are denoted $AvTMP_t^{R,M,P}$ where R is the region (1 to 7), M is the month (1 to 12) and P is the period (1986-2005, 2041-2070 or 2071-2100).

d) For each of the above time series, a time series $vIND_t^{R,M,P}$ of water stored in the IND was also extracted from corresponding SWAT simulations and used to calculate the average volume of water stored in the IND

e) The mean and standard deviation in time of $CumPCP_t^{R,M,P}$ and $AvTMP_t^{R,M,P}$ were included in a pool of potential predictors for the average in time of $vIND_t^{R,M,P}$.

f) The selection of the variables to include in the CSS was done in two steps. First, stepwise regression was used to screen the pool of potential predictors and retain only the ones which have a meaningful relation with the predictand. The two predictors that passed the screening and have the highest correlation with the predictand are finally retained as dimensions of the CSS.

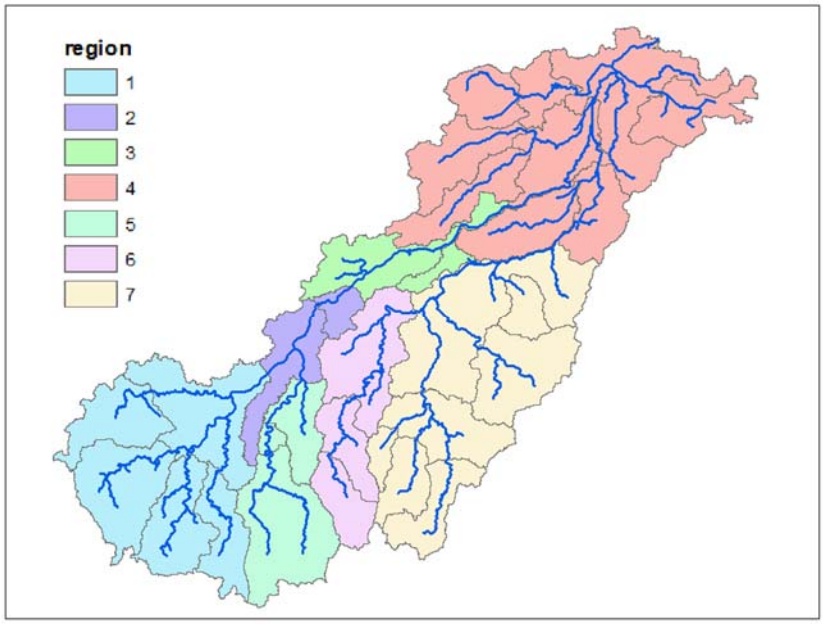

Figure 4: Regions in the UNBB

2.5 Climate Change Projections and Downscaling

The CORDEX (COordinated Regional Downscaling Experiment: Giorgi et al., 2009) aims to simultaneously evaluate global climate models and produce climate projections for use in impact and adaptation studies, mainly through dynamical downscaling. A set of 40 regional climate models outputs (20 different climate models, two RCP scenarios: RCP4.5 and RCP8.5) were obtained from the CORDEX team. The list of the regional climate models, the institution in which they were developed along with the driving Global Circulation Model (GCM) are provided in Table 1. The outputs of the RCMs were downscaled using quantile-quantile mapping following Amadou et al. (2014)

Table 1: list of Regional Climate Models used in the study

RCM	**CANRCM4**	**CCLM-4-8-17**	**CCLM-4-8-17**	**CCLM-4-8-17**	**HIRHAM5-v1**
Institution	CCCma (Canadian Centre for Climate Modelling and Analysis, Victoria, BC, Canada)	Climate Limited-area Modelling Community (CLM-Community)	Climate Limited-area Modelling Community (CLM-Community)	Climate Limited-area Modelling Community (CLM-Community)	Danish Meteorological Institute
Driving GCM	CanESM2	ICHEC-EC-EARTH	MOHC-HadGEM2-ES	MPI-M-MPI-ESM-LR	NCC-NorESM1-M
RCM	**RACMO22T**	**RCA4-v1**	**RCA4-v1**	**RCA4-v1**	**RCA4-v1**
Institution	Royal Netherlands Meteorological Institute	Swedish Meteorological and Hydrological Institute, Rossby Centre	Swedish Meteorological and Hydrological Institute, Rossby Centre	Swedish Meteorological and Hydrological Institute, Rossby Centre	Swedish Meteorological and Hydrological Institute, Rossby Centre
Driving GCM	ICHEC-EC-EARTH	CCCma-CanESM2	CNRM-CERFACS-CNRM-CM5	CSIRO-QCCCE-CSIRO-Mk3-6-0	ICHEC-EC-EARTH
RCM	**RCA4-v1**	**RCA4-v1**	**RCA4-v1**	**RCA4-v1**	**RCA4-v1**
Institution	Swedish Meteorological and Hydrological Institute, Rossby Centre	Swedish Meteorological and Hydrological Institute, Rossby Centre	Swedish Meteorological and Hydrological Institute, Rossby Centre	Swedish Meteorological and Hydrological Institute, Rossby Centre	Swedish Meteorological and Hydrological Institute, Rossby Centre
Driving GCM	IPSL-IPSL-CM5A-MR	MIROC-MIROC5	MOHC-HadGEM2-ES	MPI-M-MPI-ESM-LR	NCC-NorESM1-M
RCM	**RCA4-v1**	**REMO2009-v1**	**REMO2009-v1**	**REMO2009-v1**	**WRF331-v1**
Institution	Swedish Meteorological and Hydrological Institute, Rossby Centre	Helmholtz-Zentrum Geesthacht, Climate Service Center, Max Planck Institute for Meteorology	Helmholtz-Zentrum Geesthacht, Climate Service Center Germany	Helmholtz-Zentrum Geesthacht, Climate Service Center Germany	Uni Research and the Bjerknes Centre for Climate Research
Driving GCM	NOAA-GFDL-GFDL-ESM2M	ICHEC-EC-EARTH	IPSL-IPSL-CM5A-LR	MOHC-HadGEM2-ES	NCC-NorESM1-M

2.6 Weather Generator and Climate Time Series Likelihood Estimation

The weather generator proposed by Sharif and Burn (2007) was used to generate 250 realizations of the historical climate. This approach is based on a traditional resampling of the historical data but a random component is added to the individual resampled data points in order to reproduce values that are not in the historical records. For temperature variables, the temporal window and the number of nearest neighbor's k are arbitrarily chosen to be 14 days and 7 neighbors. It is assumed that the representation of the synthetically generated time series in the CSS will represent the natural climate variability. The density of the points can be converted into a two-dimensional probability distribution as illustrated in Figure 5, and used to assess the likelihood of other climate time series.

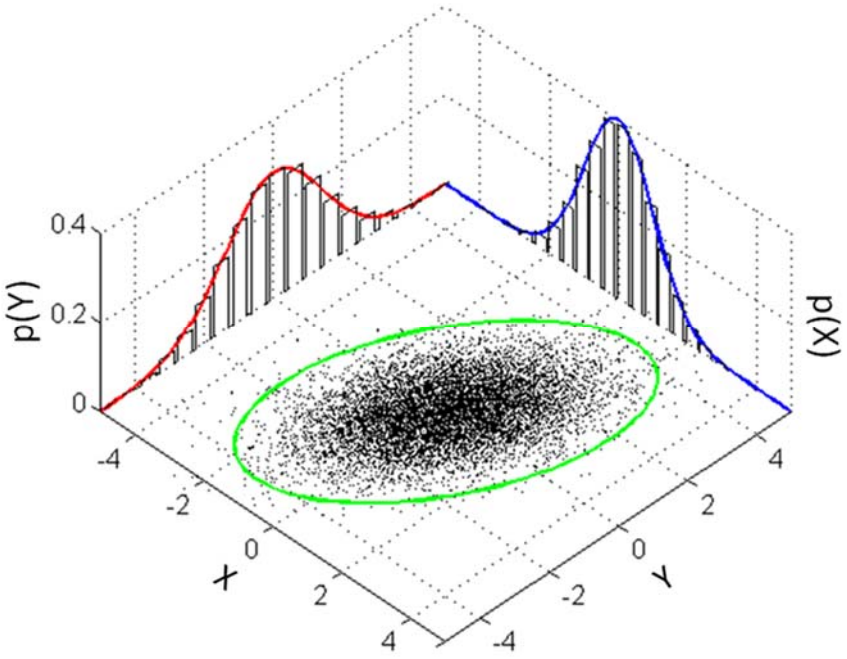

Figure 5: Illustration of the conversion of a cloud of points in a two dimensional space into a bidirectional probability density function.

2.7 Combining Weather Generator Outputs and Downscaled Climate Models Outputs To Generate High Resolution Projections

One of the major limitations of the 'top-down' approach is that the number of scenarios is too low to fully explore the risk space. The problem may be mitigated by cloning projections generated by climate models and slightly 'perturbing' them so that the new set of scenario will have the same span as the synthetic time series in the climate statistics space. The research challenge is to identify determination the 'perturbation' will be done while keeping the representativeness of the new scenario. In this paper, given an output PCP_t^{WGN} of the KNN weather generator and the perturbation is done by applying the following transformation to downscaled climate model outputs:

[2] $$PCP_t^{RCM,TR} = PCP_t^{RCM} \frac{\underset{\substack{month=month(t) \\ 1986 \le year(t) \le 2005}}{AVG} \left(PCP_t^{WGN} \right)}{\underset{\substack{month=month(t) \\ 1986 \le year(t) \le 2005}}{AVG} \left(PCP_t^{RCM} \right)}$$

Where $PCP_t^{RCM,TR}$ is the perturbed RCM output, PCP_t^{RCM} is the original RCM output, and PCP_t^{WGN} one of the outputs of the KNN weather generator. The expectation is that after transformation, the mean of $PCP_t^{RCM,TR}$ would be closer to the mean and standard deviation of $PCP_t^{RCM,TR}$ on the historical period.

$$[3] \quad TMP_t^{RCM,TR} = \underset{\substack{month=month(t) \\ 1986 \le year(t) \le 2005}}{AVG}\left(TMP_t^{WGN}\right) + \left(TMP_t^{RCM} - \underset{\substack{month=month(t) \\ 1986 \le year(t) \le 2005}}{AVG}\left(TMP_t^{WGN}\right)\right) \frac{\underset{\substack{month=month(t) \\ 1986 \le year(t) \le 2005}}{STD}\left(TMP_t^{WGN}\right)}{\underset{\substack{month=month(t) \\ 1986 \le year(t) \le 2005}}{STD}\left(TMP_t^{WGN}\right)}$$

Where $TMP_t^{RCM,TR}$ is the perturbed RCM output, TMP_t^{RCM} is the original RCM output, and TMP_t^{WGN} one of the outputs of the KNN weather generator. The expectation is that after transformation, the mean of $TMP_t^{RCM,TR}$ would be closer to the mean and standard deviation of TMP_t^{WGN} on the historical period.

3 RESULTS AND DISCUSSION

3.1 Calibration and Validation of The Hydrological Model

The hydrological model was successfully calibrated and validated on the UNBB, with NS coefficient ranging from 0.6 to 0.93 in calibration, and from 0.45 to 0.9 in validation.

Table 2: Calibration and validation performance

Hydrometric	Latitude	Longitude	Nash–Sutcliffe efficiency coefficient (NS) (validation period)	(calibration period)
Kankan	10.38	-9.31	0.8	0.65
Baro	10.51	-9.72	0.73	0.68
Kouroussa	10.64	-9.88	0.78	0.68
Banankoro	11.68	-8.67	0.9	0.86
Sélingué aval barrage	11.64	-8.24	0.64	0.45
Koulikoro	12.85	-7.56	0.93	0.87
Kirango	13.69	-6.08	0.82	0.86
Ké-Macina	13.95	-5.36	0.91	0.9
Bougouni	11.39	-7.45	0.78	0.77
Pankourou	11.44	-6.58	0.6	0.74
Douna	13.21	-5.9	0.9	0.79
Mopti	14.49	-4.21	0.78	0.8
Akka	15.4	-4.24	0.84	0.87
Diré	16.27	-3.39	0.75	0.9

3.2 Climate Change Projections and Downscaling

The 40 downscaled climate time series were used to force the calibrated SWAT model. Results show an increase in temperature ranging from 1ºC to 5.9 ºC between 2041 and 2100 (Table 3). Projected changes in precipitation (resp. water volume in the IND) range from -29% to +27.5% (-45% to 104.2%).

Table 3: range of projected changes in temperature, precipitation and water volume in the IND

	Temperature (ºC)	Precipitation (mm)	Water volume in the IND (million m^3)
Average value in 1986-2005	28.6	1001	4671
Change in 2041-2070, RCP4.5	1.0 to 2.9	-116.0 (-11.6%) to 66.3 (6.6%)	-990.6 (-21.2%) to 4867.2 (104.2%)
Change in 2041-2070, RCP8.5	2.0 to 4.6	-146.6 (-14.6%) to 89.9 (9.0%)	-1204.9 (-25.8%) to 991.5 (21.2%)
Change in 2071-2100, RCP4.5	1.2 to 3.4	-115.8 (-11.6%) to 96.1 (9.6%)	-920.9 (-19.7%) to 4216.6 (90.3%)
Change in2071-2100, RCP8.5	2.6 to 5.8	-298.2 (-29.8%) to 275.1 (27.5%)	-2102.9 (-45.0%) to 2085.6 (44.6%)

The above results show that some rather drastic changes are projected by individual models, and raises the question of the credibility of these models. In the traditional 'top-down' approach, each model in the pool is given the same credibility.

3.3 Climate Statistics Space and Climate Response Function

Using stepwise regression (entrance *p*-value=0.01; exit *p*-value=0.05), the following variables were retained as potential predictors for the average volume of water in the IND: $AVG(CumPCP_t^{1,9,*})$, $AVG(CumPCP_t^{1,9,*})$, $AVG(CumPCP_t^{3,1,*})$, $AVG(CumPCP_t^{4,1,*})$, $AVG(CumPCP_t^{6,7,*})$, $AVG(CumPCP_t^{7,10,*})$, $AVG(AvTMP_t^{4,1,*})$, $STD(CumPCP_t^{1,9,*})$, $STD(CumPCP_t^{4,1,*})$, $STD(CumPCP_t^{3,1,*})$ $STD(CumPCP_t^{4,12,*})$, $AVG(CumPCP_t^{7,6,*})$ where $AVG(CumPCP_t^{R,M,*})$ is the average of cumulative precipitation between month 1 and month M on region R, $AVG(AvTMP_t^{R,M,*})$ is the average temperature between month 1 and month M over region R, and $AVG(CumPCP_t^{R,M,*})$ is the standard of cumulative precipitation between month 1 and month M on region R. The '*' as the end means that the average and standard deviation can be calculated on any of the three periods considered in the study (1986-2005, 2041-2070 or 2071-2100). Of these 11 potential predictors, the most correlated with the average volume of water in the IND were $AVG(CumPCP_t^{6,7,*})$ and $AVG(CumPCP_t^{7,10,*})$. They were therefore retained for inclusion in the CSS. The fit of the Climate response function (a linear regression equation linking the two selected predictors and the average volume of water in the IND is presented in Figure 5, panel a. The outputs of the RCMs and the KNN-WG in the CSS are presented on Figure 5, panel b. The empirical PDF derived from the weather generator outputs is presented on figure 6, panel a along with the undisturbed RCM output. It can be noticed that a significant number of RCM outputs are in the low probability area, suggesting that only five RCM outputs should actually be used.

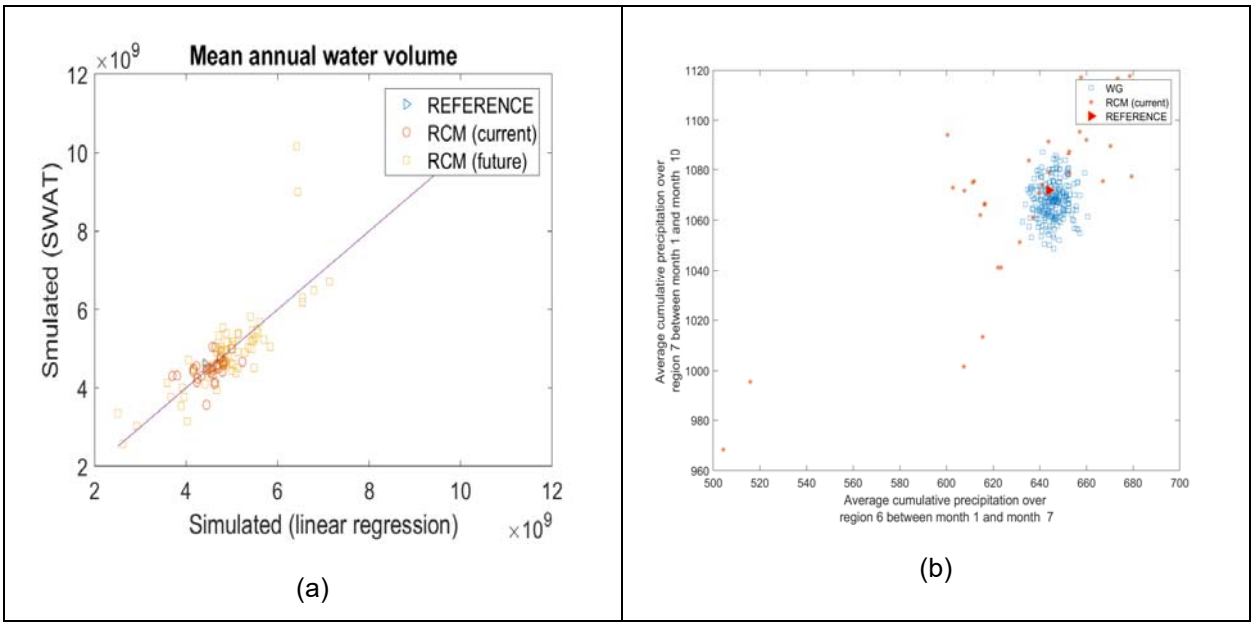

Figure 6: a) Selected Climate Response Function (Linear regression between the mean annual water volume in the IND and the two selected predictors) and b) representation of RCM outputs and synthetically generated time series in the DCC.

The magnitude of the empirical PDF can be used to set a credibility to RCM outputs both on the historical period. and future periods. This is already an improvement from the usual practice of assigning an equal weight to all RCM outputs. However, the low number of points in the high probability space may ne an issue. That's why the transformation described in section 2.7 was proposed to comb weather generator outputs and downscaled climate models outputs to generate high resolution projections. Figure 6.b shows the transformed RCM outputs after the transformation described in section 2.7. The number of projections went from 40 to 10,000 with a large number of them in the high probability area. This will allow a better coverage of potential future risks if the new time series are fed in the SWAT model of the UNBB or the Climate Response Function.

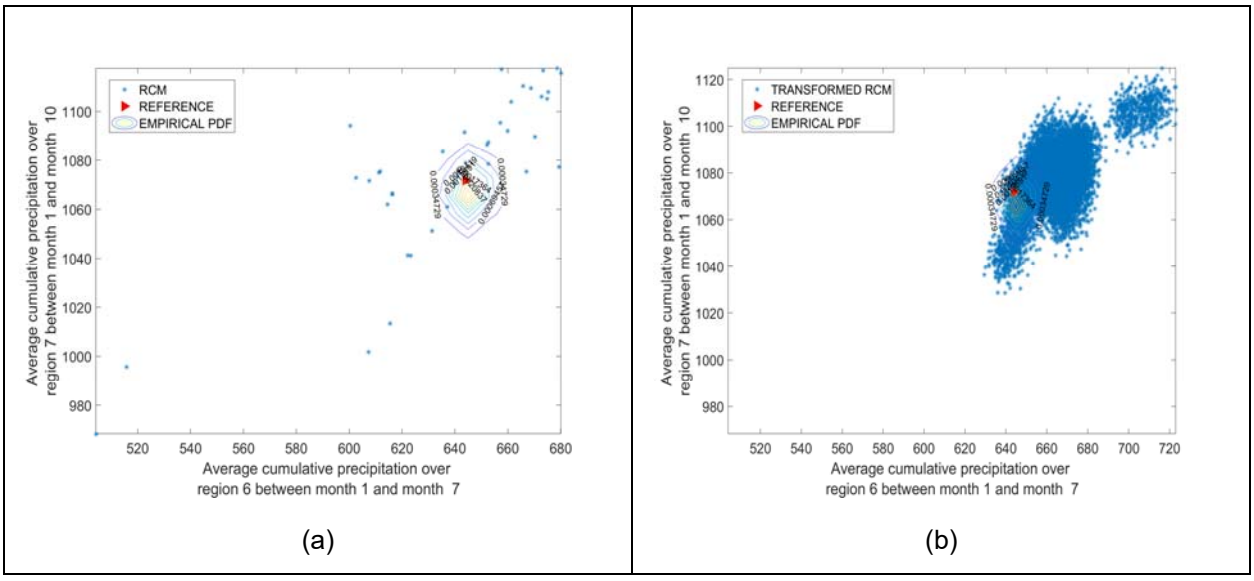

Figure 7: a) Empirical PDF and position of the RCM outputs in the CSS and b Empirical PDF and position of the transformed RCM outputs in the CSS.

Some aspects that need to be improved in the proposed methodology are a) the nature of the Climate Response Function and b) the method to combine weather generators outputs and RCM outputs so that the results cover the entire high probability region. Relationships in the climate system are usually highly nonlinear, and it is anticipated that the used of non-linear climate response functions (e.g. artificial neural networks) would lead to a better fit in the relationships between elements of the CSS and elements of the RPIS. In this paper, the cloud of transformed RCM outputs did not perfectly overlay with the cloud of the weather generator outputs in the CSS, leading to an imperfect coverage of the RPIS. Alternative transformation methods such as quantile mapping may lead to better results. Despite these limitations, the proposed methodology is considered promising and may lead to a better identification of risks associated with climate change, and better adaptation decision.

4 CONCLUSIONS

This paper highlighted the promises of the bottom-up approach to risk discovery compared to the traditional top-down approach. The limited number of RCM projections available to modellers and the lack of methodology to rank RCM outputs was identified as one of the major limitations to the application of the bottom-up approach. A new stochastic method is proposed to generate a large number of climate change projections by combining the outputs of weather generators to the outputs of regional climate models, and associate them with a likelihood value. The increased number of projections allows a better coverage of the risk space and while the likelihood value allows for a more realistic assessment of the plausibility of future risks.

References

Abbaspour, K.C. (2012). SWAT-CUP 2012: SWAT calibration and uncertainty programs. Eawag: Swiss Federal Institute of Aquatic Science and 8 Technology. Retrieved from http://www.neprashtechnology.ca.

Amadou, A., Gado Djibo, A., Seidou, O., Sittichok, K., Seidou Sanda, I. (2014). Changes to flow regime on the Niger River at Koulikoro under a changing climate. Journal of hydrological sciences. DOI: 10.1080/02626667.2014.916407

Arnold, J.G., Srinivasan, R., Muttiah, R. S. and Williams, J.R. (1998). Large area hydrologic modeling and assessment part i: model development. Journal of the American Water Resources Association, 34(1):73–89, doi: 10.1111/j.1752-1688.1998.tb05961.x.

Bartholom, E. and Belward, A.S. (2005). GLC2000: a new approach to global land cover mapping from Earth observation data. International Journal of Remote Sensing, 26(9):1959–1977, doi: 10.1080/01431160412331291297.

Brown, C, Y Ghile, M Laverty, and K Li. 2012. “Decision Scaling: Linking Bottom-up Vulnerability Analysis with Climate Projections in the Water Sector: decision scaling-linking vulnerability analysis.” Water Resources Research 48 (9): doi:10.1029/2011WR011212.

FAO/UNESCO. Digital soil map of the world and derived soil properties [online]. rev. 1 cd rom. Available online at h ttp://www.fao.org/catalog/what new-e.htm, 2003.

Giorgi, F, C Jones, and G R Asrar. 2009. “Addressing Climate Information Needs at the Regional Level: The CORDEX Framework.” Bulletin of the World Meteorologic Organization 58 (3): 175–83.

Jarvis, A., Reuter, H., Nelson, A., Guevara, E. (2008). Hole-flled srtm for the globe version 4, available from the cgiar-csi srtm 90m database (http://srtm.csi.cgiar.org).

Sharif M, Burn D H (2007) Improved K-nearest neighbor weather generating model. J Hydrol Eng 12(1):42–51

G. P. Weedon, G.P., Balsamo, G., Bellouin, N., Gomes, S., Best, M.J., and Viterbo, P. (2014). The WFDEI meteorological forcing data set: WATCH Forcing Data methodology applied to ERA-Interim reanalysis data. Water Resources Research, 50(9):7505–7514, doi: 10.1002/2014WR015638.

Stainforth, D A, T E Downing, R Washington, A Lopez, and M New. 2007. “Issues in the Interpretation of Climate Model Ensembles to Inform Decisions.” Philosophical Transactions of the Royal Society A: Mathematical, Physical and Engineering Sciences 365 (1857): 2163–77. doi:10.1098/rsta.2007.2073.

Taylor, K E, R J Stouffer, and G A Meehl. 2012. “An Overview of CMIP5 and the Experiment Design.” Bulletin of the American Meteorological Society 93(4): 485–98. doi:10.1175/BAMS-D-11-00094.1.